NASA Contractor Report 181842

Feasibility of Predicting Performance Degradation of Airfoils in Heavy Rain

(NASA-CR-181842) FEASIBILITY OF PREDICTING PERFORMANCE DEGRADATION OF AIRFOILS IN HEAVY RAIN Final Report (Continuum Dynamics) 44 p CSCL 01A

N89-25973

Unclas
G3/02 0223906

A. J. Bilanin
T. R. Quackenbush
A. Feo

Continuum Dynamics, Inc.
Princeton, New Jersey 08543

Contract NAS1-18302
June 1989

NASA
National Aeronautics and
Space Administration

Langley Research Center
Hampton, Virginia 23665-5225

TABLE OF CONTENTS

NOMENCLATURE

C_D	-	drag coefficient
D	-	droplet ejecta diameter
D_i	-	incoming droplet diameter
D_t	-	target diameter
h	-	film height
N	-	number of ejected droplets
R	-	droplet ejecta radius
U	-	ejecta/air average velocity
$\overline{U}$	-	boundary layer reference velocity
V_i	-	incident drop velocity
V_r	-	ejecta velocity
W_L	-	liquid water content
x	-	streamwise direction
α_r	-	reflected angle
β	-	droplet incidence angle
ε	-	fraction of incoming droplet which splashes back
λ	-	ejecta interaction layer thickness
μ_w	-	absolute viscosity of water
ρ	-	average ejecta/air density
ρ_a	-	density air
ρ_w	-	density water
σ	-	surface tension between air and water

1. INTRODUCTION

The following report documents the effort undertaken by Continuum Dynamics, Inc. on behalf of NASA Langley in support of the heavy rain aerodynamic performance penalty program. This effort supported the design of a fullscale test program as well as examined the feasibility of estimating the degradation of performance of airfoils from first principles. The analytic efforts were supplemented by a droplet splashback test program in an attempt to observe the physics of impact and generation of ejecta. These tests demonstrated that the interaction of rain with an airfoil is a highly complex phenomenon and this interaction is not likely to be analyzed analytically with existing tools.

In 1985, Bilanin (Ref. 1) undertook a scaling analysis to determine if subscale test results, which were being obtained in Langley's VSTOL tunnel, could be extrapolated to fullscale. It was concluded that it was likely that viscous and surface tension phenomenon both played a role in the performance degradation observed at subscale and extrapolating these results to fullscale was indeed risky. The following report examines viscous and surface tension phenomenon in the hope of illuminating the complex rain splash-boundary layer interaction.

2. SPLASHBACK / BOUNDARY LAYER ANALYSIS

To support experimental work on the effect of heavy rain on the behavior of airfoil boundary layers, a computational effort was undertaken with the objective of assembling software to simulate the effect of droplet impingement on airfoil flowfield boundary layer separation. The features selected for the analysis were chosen to allow realistic variations in the incident flow, droplet size, and pressure gradient on the airfoil. The analysis proceeds by 'smearing out' many features of the incident rainfall and the subsequent splashback, an appropriate approach given the difficulty of characterizing the details of droplet impact.

The discussion that follows will first describe the flat-plate boundary layer code that served as the foundation of this analysis, as well as the preliminary test runs that were undertaken to validate it. Then the basics of the rainfall model used in the simulation will be outlined, with particular attention to the inputs required and the assumptions made. The effect of representative heavy rain situations on the boundary layer behavior will be described, and a discussion of the required input parameters fixes the ground work for a splashback experiment.

2.1 Parabolic Boundary Layer Analysis

The starting point for this investigation of the effect of heavy rain on boundary layer separation was the examination of the behavior of a 'dry' boundary layer flow over a flat plate. Ultimately, this 'dry' analysis was supplemented with the imposition of longitudinal pressure gradients representative of those experienced on airfoils of commercial transports in landing configuration. To begin, however, the fundamental features of the baseline analysis will be described.

Development began with an existing simulation program for a shear layer in an incompressible fluid. The program carried out a parabolic evolution of the velocity profile over the plate using an implicit time-marching scheme. The model included the effect of turbulent transport of momentum via a second-order-closure model very similar to that described in References 2 and 3. The analysis included a provision for variable time steps as well as for the automatic remeshing of evaluation points in the velocity profile so as to maximize the use of points in those parts of the profile featuring steep gradients.

The first step was to impose appropriate boundary conditions on the flow to convert the simulation to a model of a surface boundary layer. In this new format, the program required as input the incident velocity profile, the kinematic viscosity, the elapsed time to be simulated, and the maximum number of points to be used in the profile. Terms were also added to include the effect of a pressure gradient in the free stream.

As an initial check, the coefficients governing the turbulent transport model were suppressed and the evolution of the boundary layer in laminar flow was observed. In this mode, the program correctly recovered the Blasius laminar boundary layer solution. With the coefficients replaced, quantitatively reasonable boundary layers were recovered, as well. To examine the program's handling of the onset of separation, adverse pressure gradients in the free stream were imposed. These cases also produced the expected qualitative behavior, i.e. the boundary layer thickened considerably and the velocity gradients near the wall increased relative to the laminar case. In sum, these sample 'dry' runs achieved their objective of enhancing confidence in the baseline analysis and in laying the groundwork for the implementation of the rain model.

2.2 Model of Heavy Rain in the Boundary Layer

The principal method of coupling the effect of the impingement and splashback of raindrops on the boundary layer was via the imposition of an effective drag force in momentum equation. The physical mechanism involved was modeled as follows: first, a given flux of rain was assumed to penetrate a layer of specified thickness (not necessarily equal to the boundary layer thickness, but of the same order) near the airfoil surface. This influx was then assumed to splash into droplets of a pre-determined radius and drag coefficient and to remain trapped within the specified layer for the remainder of the calculation. The shattered drops were assumed to be smeared over the full height of the layer and to move with a uniform velocity U. By advancing the two simple governing equations shown in Figure 1 in the time-like variable x, the evolution of the drag force exerted by the drops on the air in the boundary layer could be tracked through the changes in U. This drag force was applied uniformly across the full thickness of the boundary layer and constituted a simple model of the coupling of the behavior of the droplets and the airstream near the surface.

As is evident from Figure 1, this model requires the selection of a variety of parameters. The air and water density are known, and the droplet drag coefficient may be reasonably estimated given the assumption that spherical droplets result from the impact of the rain. A single droplet radius is assumed, though in actuality a wide range of droplet sizes will result from the impingement of the rain. It is also presumed that the user can specify the ambient liquid water content (W_L) in the atmosphere. The incident raindrop speed V_i is determined from the terminal velocity of the rain as well as the airspeed of the aircraft. The resultant velocity of the incident drops relative to the surface of course depends on the flight path of aircraft, and this information is contained in the angle β. This angle also contains the influence of the surface curvature, i.e. the surface is kept flat for the purpose of calculation but the incidence angle is changed as a function of the local slope.

Two other parameters need to be specified to complete this simplified, smeared model. The first of this is the droplet layer thickness λ. When this thickness is taken to be of the same order as the boundary layer thickness, strong coupling is expected. The final parameter is the reference velocity of the air. In reality, after splashback droplets will leave the surface with a wide range of velocities, but it will be their velocity relative to the air around them that will determine whether they will accelerate or decelerate the local flow. It would be possible in principle to allow the drag force to vary in the direction normal to the surface by referencing the local drag contribution to the velocity at a given height in the boundary layer, but it was judged to be more consistent with the 'smeared' nature of this model to use a single reference velocity equal to a substantial fraction of the free stream speed to determine the drag contribution.

2.3 Sample Calculations with Rain

To test the performance of this model, several calculations were undertaken using input parameters representative of a full-scale jet transport in landing configuration. The objective of these calculations was to see if the presence of realistic rain levels produced noticeable acceleration of separation from the airfoil surface. These calculations incorporated not only the droplet and boundary layer models described above, but also included the free stream pressure gradient and surface slope of an NACA 64210 airfoil;

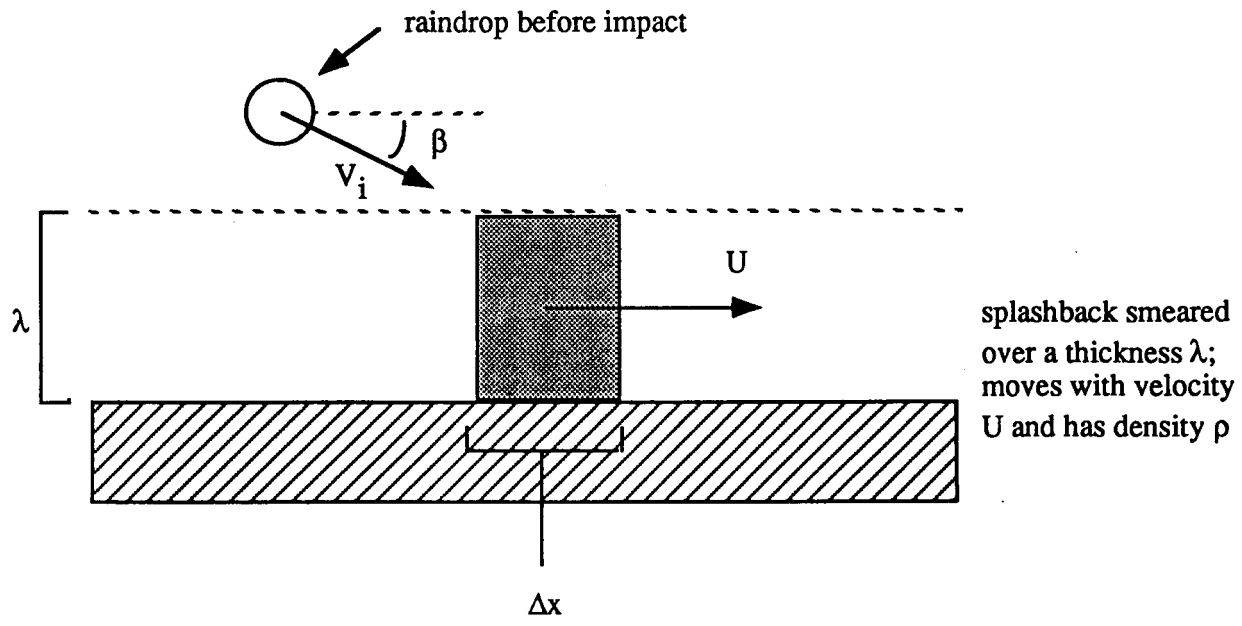

W_L = free stream LWC
C_D = droplet drag coeffcient
ρ_a = air density
ρ_w = water density
R = droplet radius after splash
$\overline{U}$ = reference velocity

Continuity Equation:

$$\frac{\partial}{\partial x}\left[\rho U\right] = \frac{W_L V \sin\beta}{\lambda}$$

Momentum Equation:

$$\frac{\partial}{\partial x}\left[\rho U^2\right] = \frac{3}{4}\left[\frac{C_D \rho_a}{R\,\rho_w}\right]\rho\,(\overline{U}-U)\left|\overline{U}-U\right| + \frac{W_L V_i^2 \sin\beta\cos\beta}{\lambda}$$

drag force term

Figure 1. Rain model and transport equations.

these quantities were computed with a separate airfoil simulation and used as input to the current analysis.

The results of one such calculation are shown in Figure 2, which plots the velocity profile at a fixed distance downstream of the leading edge of a section of a hypothetical full-scale wing. This calculation assumed a free stream velocity of 60 m/s (corresponding to the landing speed of a typical commercial transport) and an ambient liquid water content of $0.08 \frac{gm}{m^3}$. The incident rainfall impacted at an angle β of roughly 11 degrees, though this varied along the airfoil due to the surface slope. The thickness of the droplet layer was selected to be 0.003 m (thick layer), and the drag coefficient of the droplets in the splashback ejecta was estimated to be 1.0 .

Figure 2 shows the flow velocity in the boundary layer plotted against height for cases with and without rain present. Both profiles were taken at a point corresponding to a distance 10 percent downstream of the leading edge of this hypothetical airfoil (i.e., 0.40 m for a nominal 4.0 m chord). Note that the velocity profile for the case with rain present is noticeably flatter at this point than the 'dry' case, indicating that the separation process has been considerably accelerated by the presence of heavy rain.

The above model, though admittedly simplistic, contains the essential elements of droplet splashback/boundary layer interaction. The following parameters must be estimated from either observation or additional analysis:

- R - droplet ejecta radius
- λ - ejecta layer interaction thickness
- W_L - liquid water content that splashes back

2.4 Integral Analysis of Splashback

In this section an integral model of ejecta splashback is derived to help estimate ejecta diameter, interaction layer thickness λ and mass splashed back. The assumptions used in this analysis are based on the following observation from INTA's studies of splashback (Ref. 4).

- o Droplets splashback in an annular cone with large cone angle.

In Figure 3 is shown the schematic of a splash resulting from a droplet of diameter D_i and velocity V_i impacting a rigid surface at angle β . It is assumed that the ejecta droplets are reflected at angle α_r in a cone of angle α_s and the droplets are found in the spray cone annular angle $\Delta\alpha$. Conservation of mass requires that

$$\varepsilon = N\frac{D^3}{D_i^3}$$

N is the number of droplets of diameter D which are ejected and ε is the fraction of the incoming liquid which does splash. Conservation of energy requires that

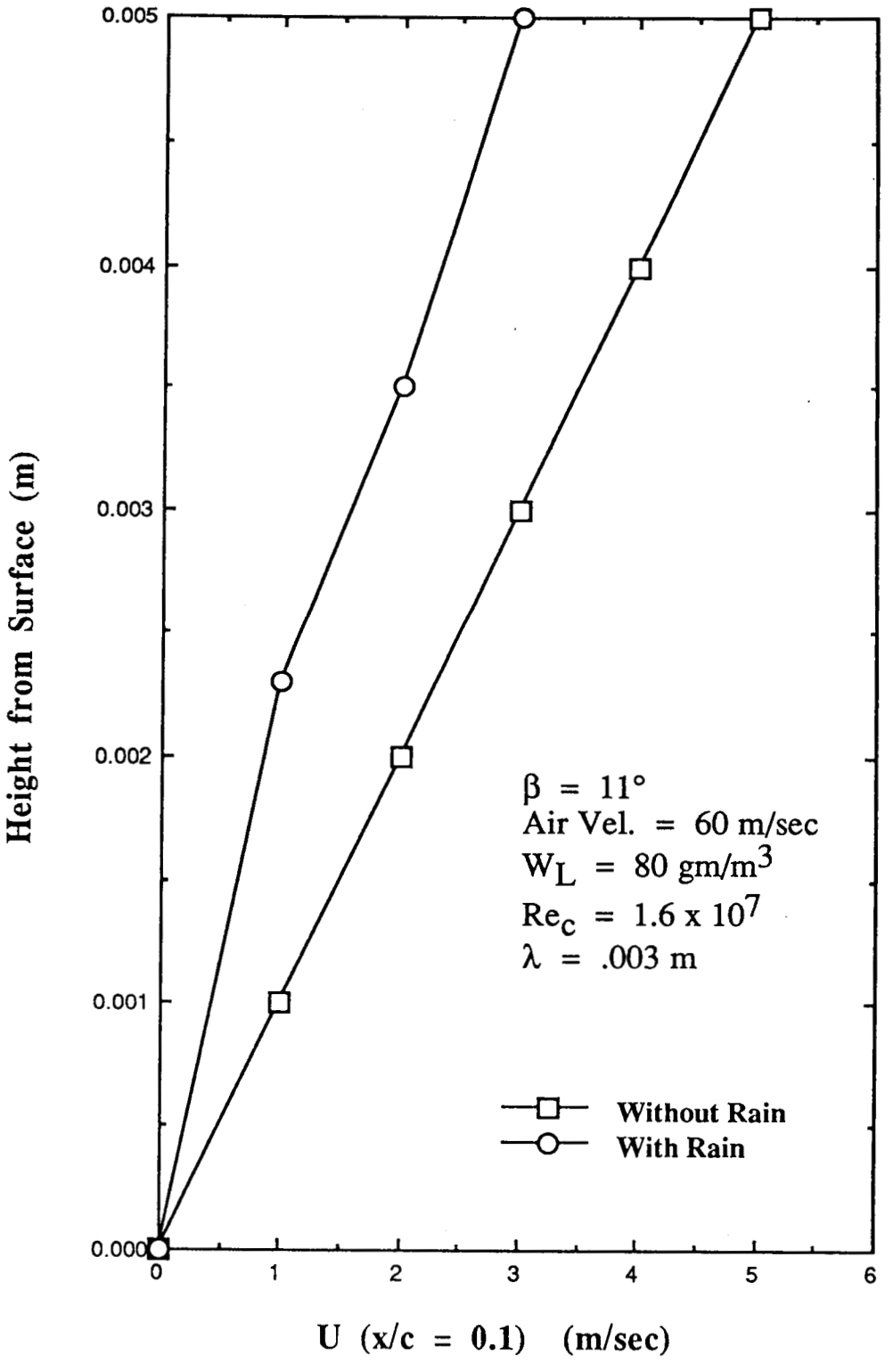

Figure 2. Velocity profile near the surface of an airfoil interacting with rain.

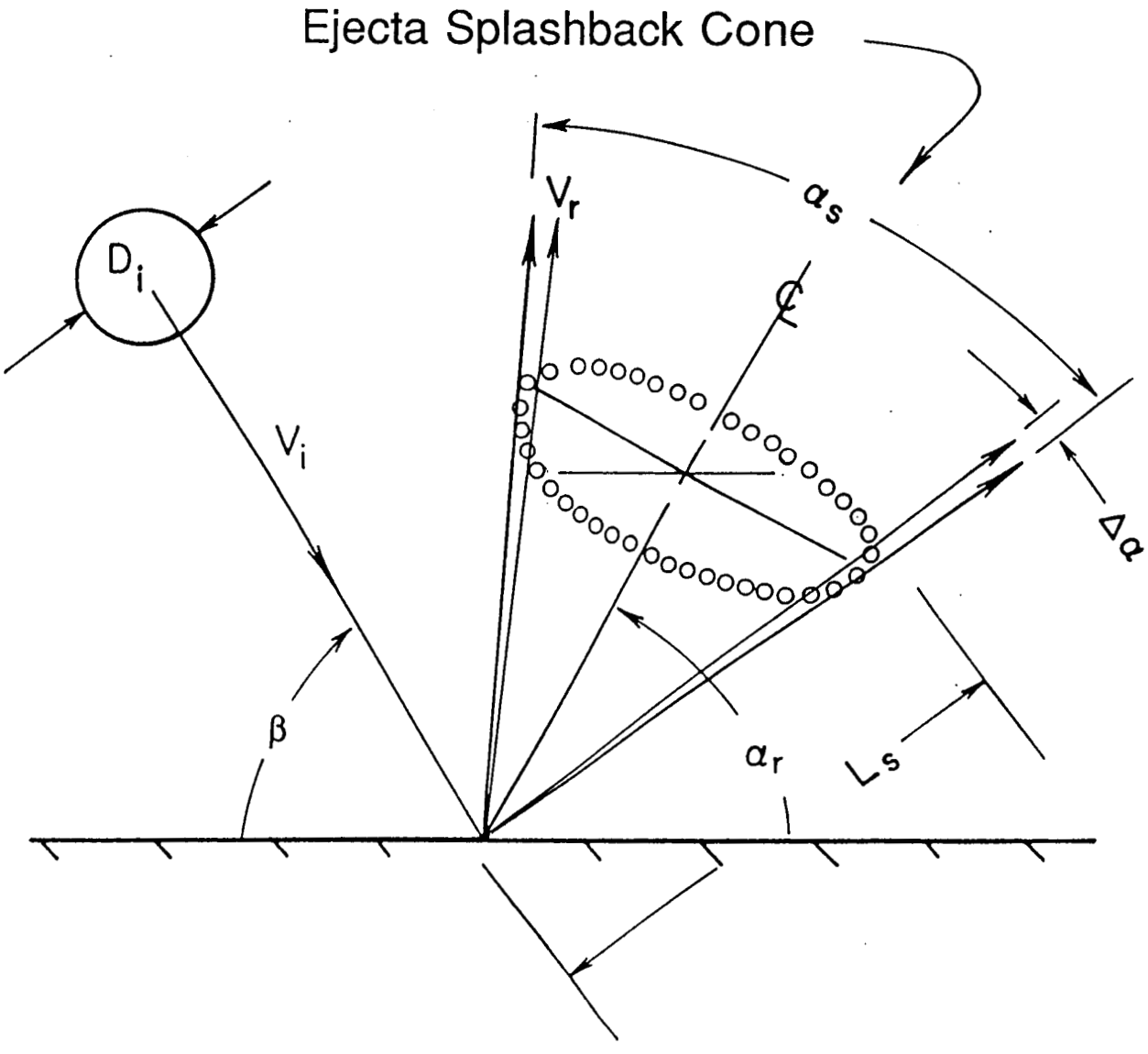

Figure 3. Schematic used in the integral analyses of droplet splash back.

$$\frac{4}{3}\pi\frac{D_i^3}{8}\frac{\rho_w}{2}V_i^2 + \sigma 4\pi\frac{D_i^2}{4} =$$

incoming k.e. surface energy

$$N\left(\frac{4}{3}\pi\frac{D^3}{8}\frac{\rho_w}{2}V_r^2 + \sigma 4\pi\frac{D^2}{4}\right)$$

outgoing k.e surface energy

where σ is the surface tension between air and water. In general the surface energy of the incoming droplet is much smaller than the kinetic energy and it is neglected in what follows.

Writing the momentum for the incident and reflected momentum as M_i and M_r respectively, then

$$\vec{M_i} = \rho_w \frac{4}{3}\pi\frac{D_i^3}{8}\vec{V_i}$$

$$\vec{M_r} = \varepsilon\frac{4}{3}\rho_w\frac{D_i^3}{8}\frac{\vec{V_r}}{2}\left(\frac{\sin^2\frac{\alpha_s}{2} - \sin^2\left(\frac{\alpha_s}{2} - \Delta\alpha\right)}{\cos\left(\frac{\alpha_s}{2} - \Delta\alpha\right) - \cos\frac{\alpha_s}{2}}\right)$$

Conserving momentum perpendicular and parallel to the surface yields

$$\beta = \alpha_r$$

$$\frac{V_r}{V_i} = 2\frac{\left(\cos\left(\frac{\alpha_s}{2} - \Delta\alpha\right) - \cos\frac{\alpha_s}{2}\right)}{\sin^2\frac{\alpha_s}{2} - \sin^2\left(\frac{\alpha_s}{2} - \Delta\alpha\right)}$$

and substituting into the energy balance yields

$$\frac{V_i^2 D\rho_w}{12\sigma} = \frac{1}{\frac{1}{\varepsilon} - \frac{V_r^2}{V_i^2}}$$

The above three expressions contain the results of this analysis. The first result which is not surprising is that the incidence angle equals the mean splash angle α_r if the collision is elastic as was assumed. The second result is much more interesting and is illustrated by examining the plot of the speed ration V_r / V_i as a function of splash cone and α_s and spray angle $\Delta\alpha$ in Figure 4. Note that to have observed speed ratios of the order of 2 or greater splash cone angles of greater than about 140° are required. Also the spray ejecta must be confined to a narrow annular region ($\Delta\alpha \sim 10° - 20°$). These observations which are based on the experimental observation of $V_r / V_i > 1$ therefore anticipate that impacting rain droplets will splash out along the surface they impact and, therefore, can potentially interact *very* strongly with the boundary layer. Assuming an elastic collision the diameter of the ejected droplets is shown on Figure 5 where the mass ejected ϵ is a parameter. Note that for large splash angles about 10% of the mass is shown to be ejected and

$$\frac{D\rho_w V_i^2}{12\sigma} \approx \mathcal{O}(1)$$

At $V_i \sim 140$ kts ejecta droplets are small and are of the order of several μ_m . By examining the volume of the ejecta cloud in the conical annular area and requiring that to be greater than the incoming volume of $\frac{4}{3}\pi\frac{D_i^3}{8}$ gives a realizability condition shown on Figure 6. Here splashes below the lines of constant $\Delta\alpha$ are realizable. This result again states that at larger splash angles only about 20-30% of the incoming mass is expected to be ejected.

These results, admittedly from a very simplistic model, hint at the difficulty in understanding the droplet impact/splashback problem.

- Ejecta droplets are of very small diameter ($\mathcal{O}(\mu m)$) and if as observed have $V_R > V_i$ are ejected at large cone angles and can therefore very effectively interact with the boundary layer.

- If the above is true, significantly more mass remains on the surface than is ejected and the airfoil lift degradation problem is complicated by film dynamics and resulting surface roughness. Hence, performance degradation may be more a boundary layer/airfoil roughness interaction than an ejecta boundary layer interaction as was first thought or as was analyzed in Reference 5.

- If the surface roughness resulting from film dynamics plays a dominant role in the observed performance degradation analytic/computer models will not likely predict this degradation from first principles.

With the above observations we have approached dynamic tests of splashing cautiously.

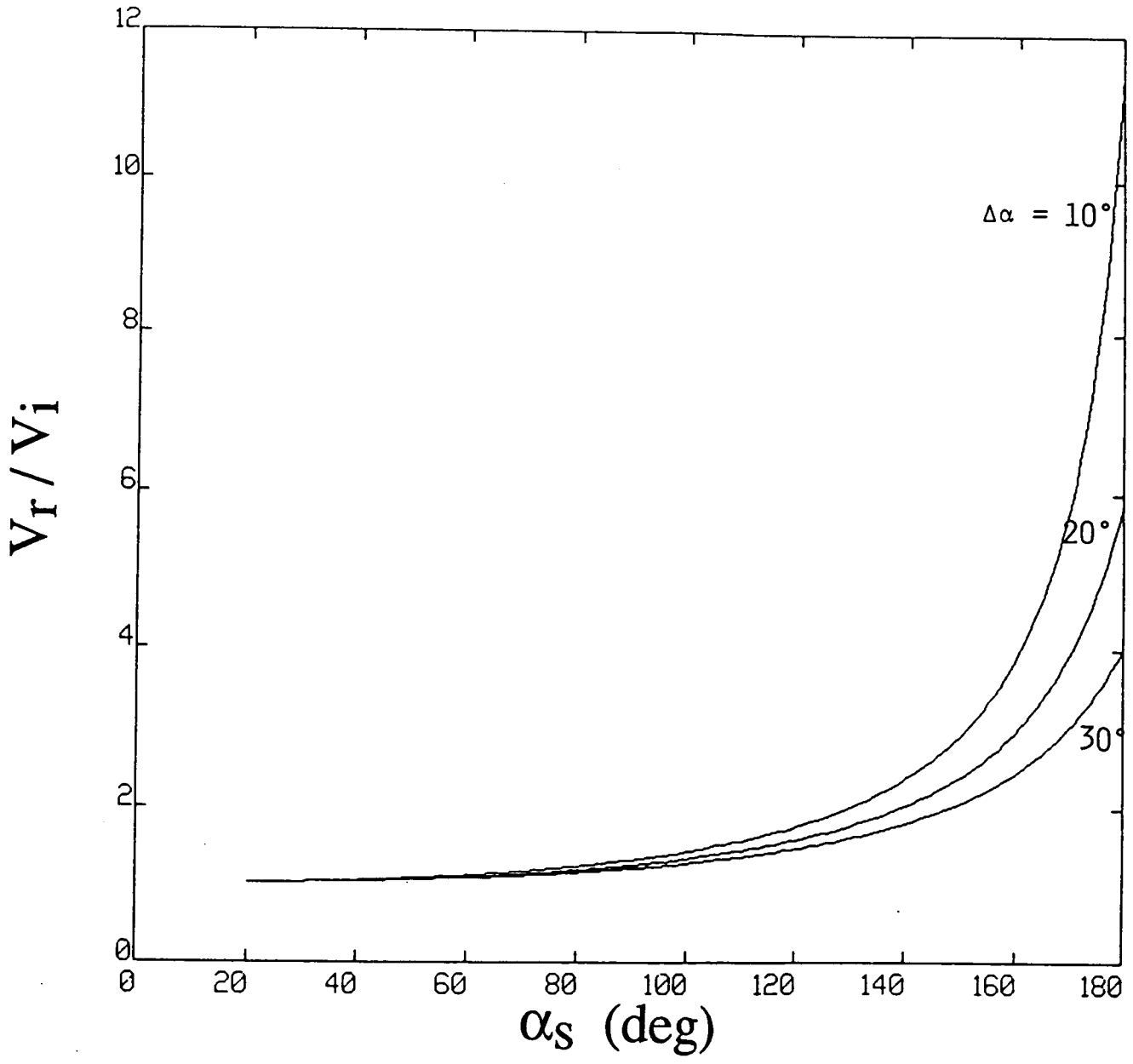

Figure 4. Speed ratio of ejected droplets as a function of spray cone angle and cone annular angle.

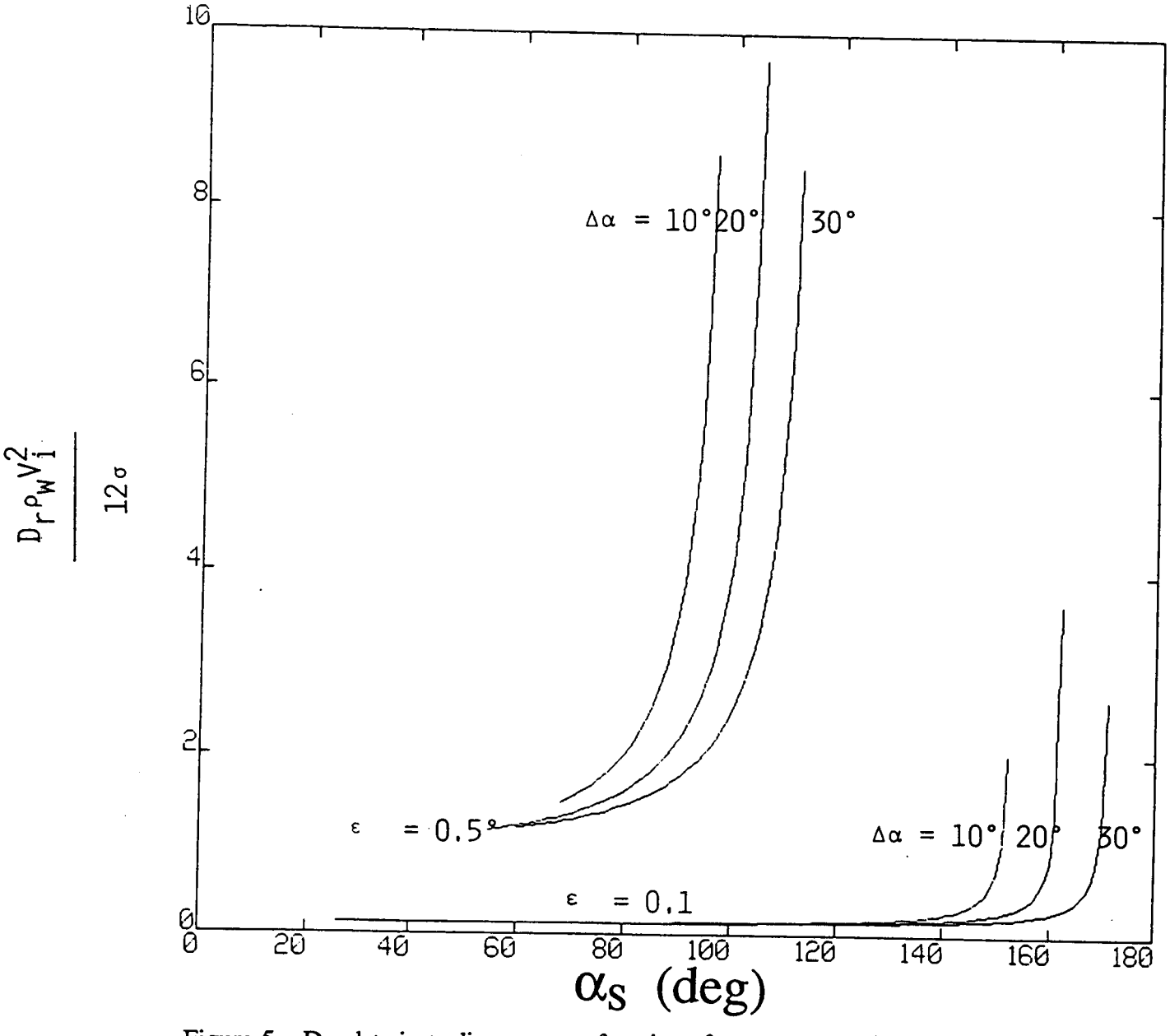

Figure 5. Droplet ejecta diameter as a function of spray cone angle and mass fraction ejected.

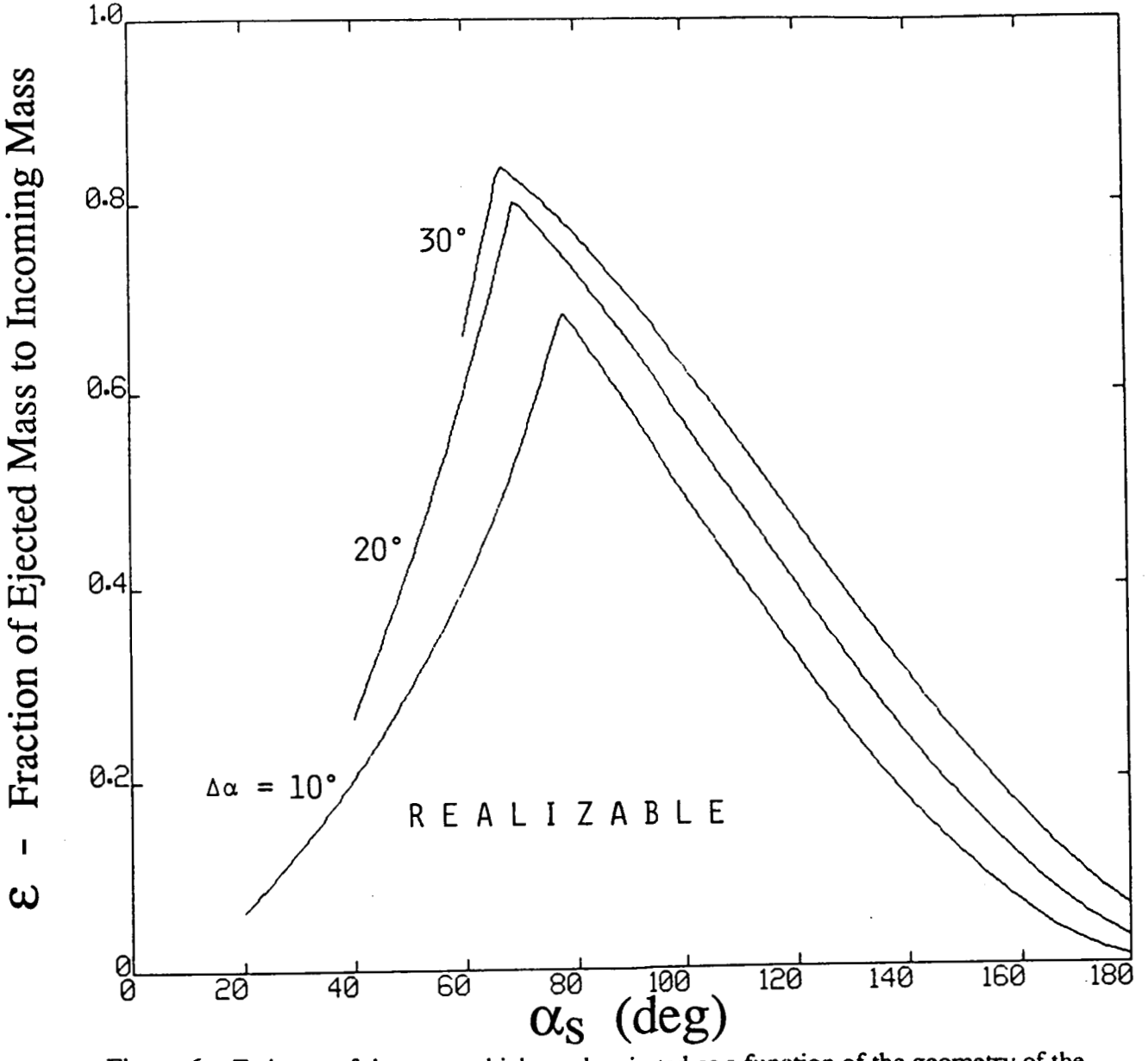

Figure 6. Estimate of the mass which can be ejected as a function of the geometry of the splash back cone.

3. EXPERIMENTAL ANALYSIS OF DROPLET IMPACT

An experimental program consisting of photographic micro analysis of the complete splashback for a single droplet impacting normal to a surface is described here. The experiments were carried out both by C.D.I. personnel as well as by staff from INTA during their working visit to C.D.I. in the fall of 1986 and the summer of 1987. The apparatus for conducting the impact tests was built during the summer of 1986 and the operation of the facility is described below.

The apparatus centers around an existing 15 hp variable speed drive unit and the configuration of the rotating arm is shown on Figure 7 (see Ref. 6 for more documentation). Drops are produced periodically, which fall under gravity and impact a rotating arm on the end of which is mounted a target. The target was either a 0024 airfoil or a series of flat-faced models two of which are shown on Figure 8. The difficulties encountered were enormous, and were associated with timing/triggering and photographing the resulting splashback ejecta. Although ultimately a technique was developed that was successful in obtaining photographic data that could be analyzed quantitatively, the detail was not sufficient to even crudely estimate the amount of mass ejected although the photographs were quite spectacular.

In Figure 9 is shown splashback of a droplet impacting the leading edge of a 0024 airfoil moving at 30 m/s (upper photograph). Although the ejecta is very visible, the technique used did not accurately allow the delay between impact and illumination to be controlled to examine subsequent impacts at earlier or later known times after impact. This is clear from the lower photograph where the test remnants of an earlier impact are still apparent and a droplet which is about to be impacted is seen above the leading edge. The photographs in Figure 9 were made by monitoring drop position and arm position using a laser beam and position switch respectively. Because of unknown random timing errors, which may be attributed to the non-constant rotation of the arm, this approach was abandoned after no method could be determined to reduce the magnitude of randomness in triggering the illumination. Although photographs of impact could always be obtained this hardware configuration could not produce a timed sequence of impact photographs (see Ref. 7).

3.1 Drop Generation and Synchronization

An alternate triggering methodology was devised by INTA (see Ref. 7) and was implemented on the C.D.I. rotating arm rig as follows.

Drops are generated by free falling from a nozzle connected to a small water reservoir, with gravity supplying the pressure needed for the drops to leave the nozzle exit. This nozzle is located in a position so that the drop strikes the model at the uppermost side of its trajectory. The nozzle exit is located 368 mm from the impact point which means that the drop has approximately a vertical velocity of 2.5 m/s at that point. This means a small deviation from a 90° incidence, but the relation between normal and tangential velocity components is small and will be ignored.

Two different nozzles have been used to generate 5 mm and 3 mm drops. For each of them a maximum rate of 400 to 300 drops/minute was obtained. A 35 mm diameter tube was used to protect the falling drops from the turbulent model wake effects.

There will not be a drop impact each time the model passes through the camera field of view and since we are only interested in impacts at the center of the model, a certain

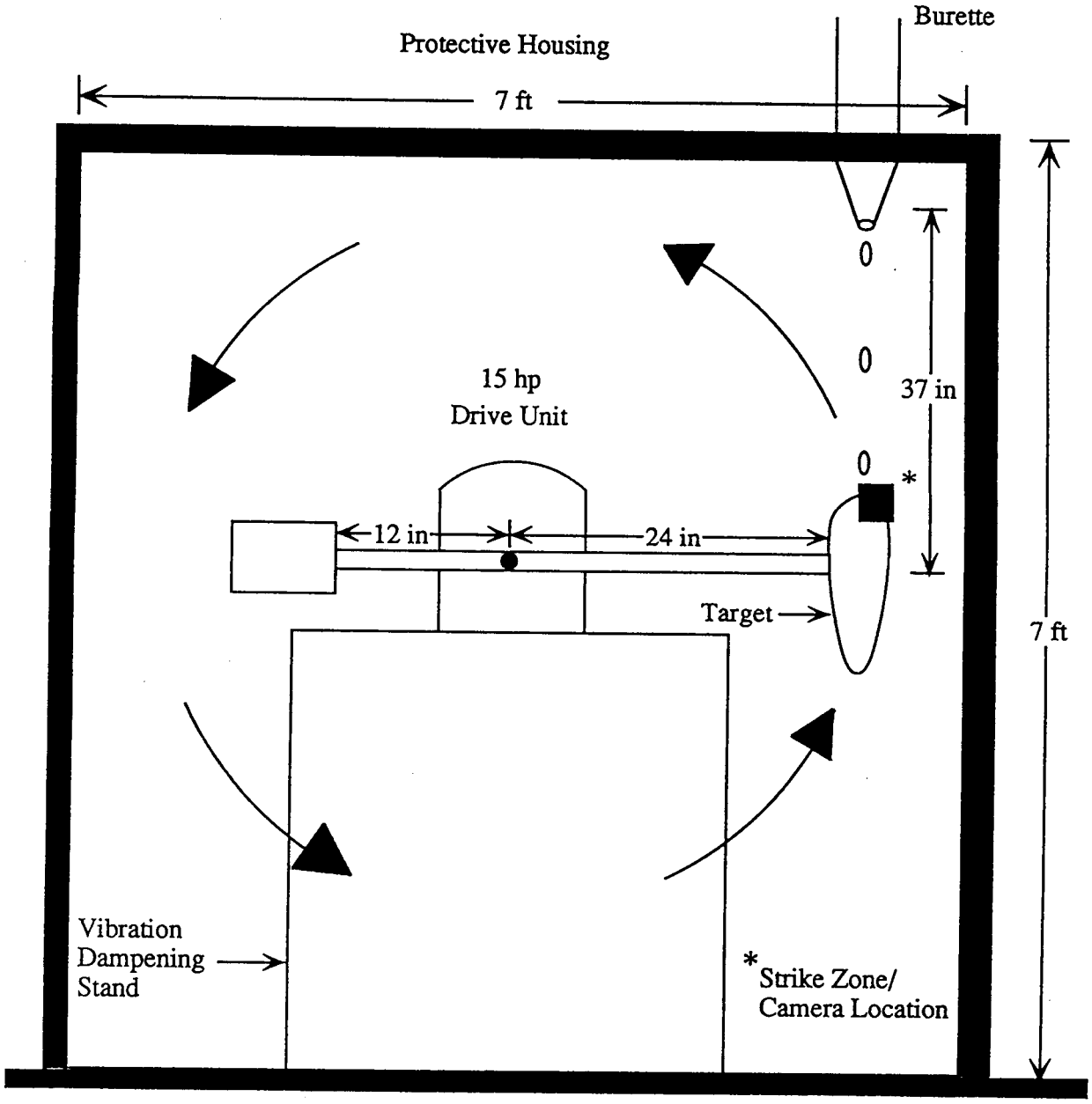

Figure 7. Rotating arm impacting.

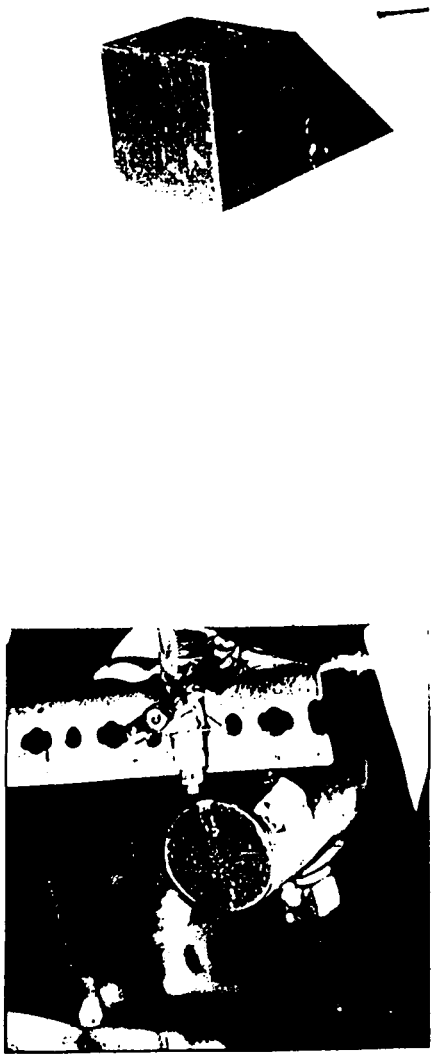

Figure 8. Flat faced impact models.

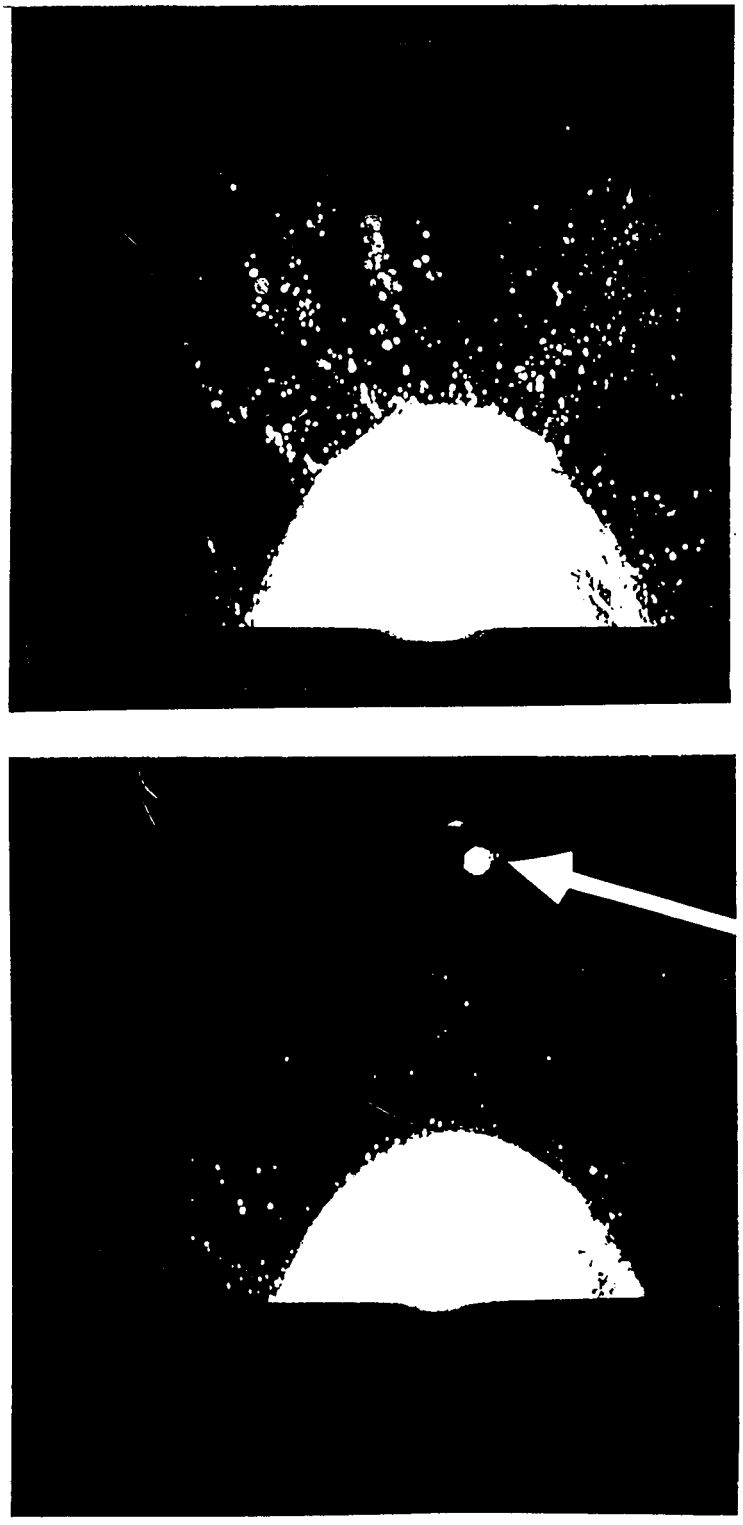

Figure 9. Ejecta splash back from a 0024 airfoil at random times after impact. Note incoming droplet in lower photograph.

synchronization is required to trigger a pulse that will activate the short duration high-intensity lamp. This synchronization is obtained by the use of two appropriately located sensors whose signals are integrated electronically, triggering a pulse when there is coincidence between them. This is schematically shown in Figure 10, where the actual delays used and also the "windows" employed are indicated. The narrower the "windows" the more exact the location of drop and model for timing reference purposes, but also the longer the wait until the occurrence of the event. With the numbers indicated an acceptable compromise was reached.

3.2 Single Picture High-Speed Photography

The pulse triggered by the synchronization system fires the lamp of a General Radio Strobotac which has been used at its maximum intensity with a duration of 5 μs . The light loses part of its intensity with distance and the lamp had to be used as close to the object as possible. The photographic camera used was a Hasselblad with an extension bellows, which permitted magnifications around 1 . The film used was a very fast (20,000 ASA) Polaroid film (type 612), to test initially if the light reflected by the phenomena was sufficient, and finally a TMAX 400 Kodak film for all the results that are presented in this report.

3.3 Description of Experiments

The objective for this set of experiments has been to obtain drop perpendicular impact information on models moving through air at their stagnation point position. The model dimensions have been chosen so that they can accommodate the splash main features, but they were not designed large enough so that the complete process could be studied until it is finished without having some target end effects.

Data has been obtained for impacts on dry as well as on wetted surfaces that have very thin films deposited. Drop diameter and drop-model relative velocity has also been changed; then difference in characteristics should be reflecting differences in the parameters

$$We_D = \frac{\rho_w V_i^2 D_i}{\sigma} \quad , \quad Re_D = \frac{\rho_w V_i D_i}{\mu_w} \quad \text{and} \quad \frac{h}{D} \quad ,$$

The following tests were performed:

Impact on a dry surface

A) $V_i = 25$ m/s ; $D_i = 3$ mm give $We_D = 2.7 \times 10^4$; $Re_D = 7.5 \times 10^4$

B) $V_i = 40$ m/s ; $D_i = 3$ mm give $We_D = 6.9 \times 10^4$; $Re_D = 1.2 \times 10^5$

Impact on a wetted surface

C) $V_i = 25$ m/s ; $D_i = 5$ mm give $We_D = 4.5 \times 10^4$; $Re_D = 1.25 \times 10^5$

D) $V_i = 40$ m/s ; $D_i = 3$ mm give $We_D = 6.9 \times 10^4$; $Re_D = 1.2 \times 10^5$;
$h/D_i = 3.3 = 0.33 \times 10^{-2}$ (estimated)

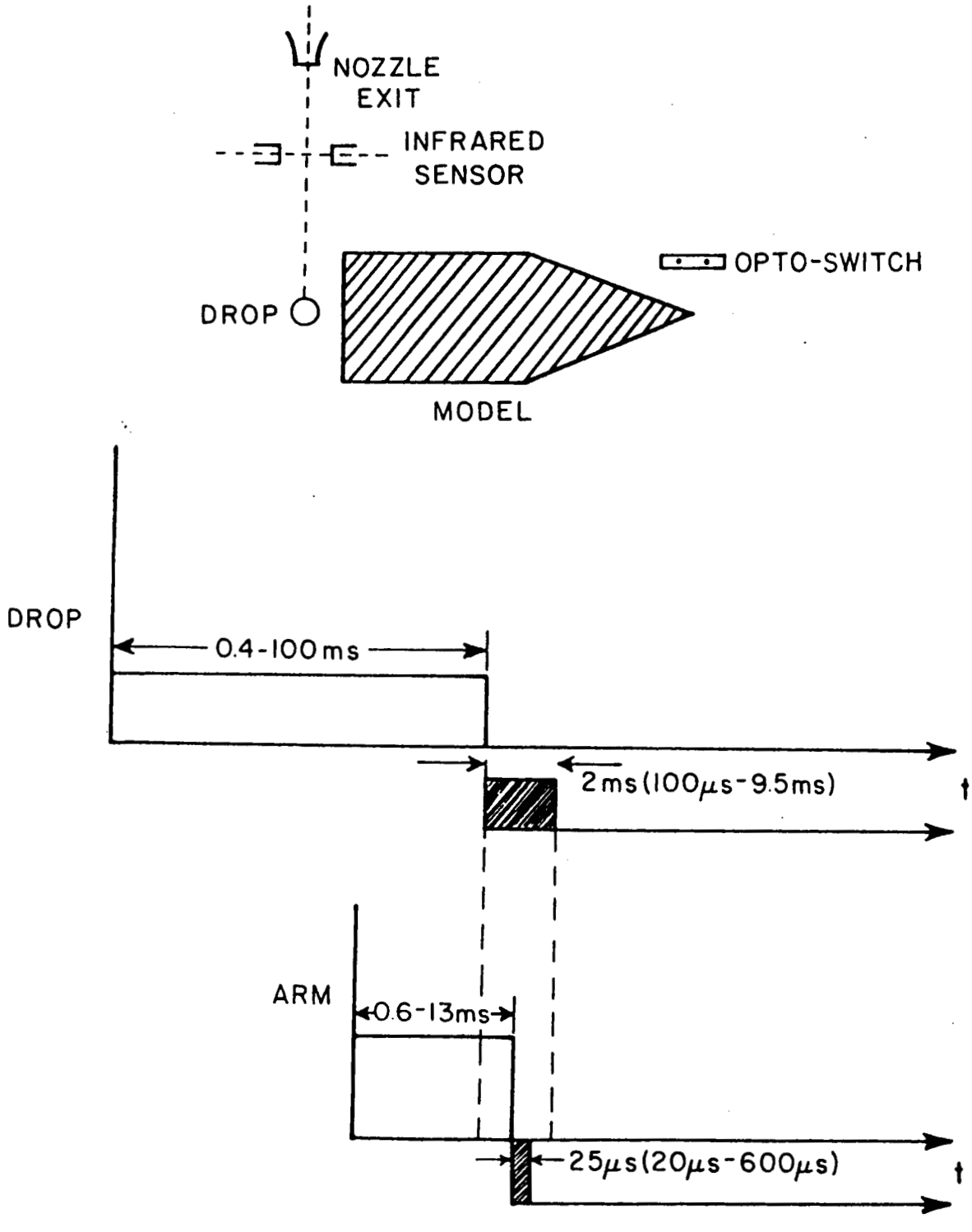

Figure 10. Synchronization by coincidence of drop and arm pulses.

$h/D_i = 3.3 = 0.33 \times 10^{-2}$ (estimated)

The film thickness in case C is not estimated because it is the result of a random number of surface impacts, whereas in case D it was produced by the model hitting a 3 mm water jet that was deliberately located past the impact location under study. The estimation in this case assumes that 50% of the water cylinder intercepted by the model is actually deposited on its surface, spreading uniformly. Then:

$$0.5 \times \frac{\pi}{4} d^2 D_t = \frac{\pi D_t^2}{4} h$$

$$h = 0.5 \frac{d^2}{D_t}$$

For $D_i = 3$ mm and $D_t = 50$ mm, the film thickness is $h = 0.09$ mm. This is considered an upper limit, since the jet is broken before it is hit by the model and water is lost in one revolution by air shear stresses and centrifugal forces. The lower limit taken is the smaller practical thickness that the film could have in nominal conditions before it breaks up ($h \sim 0.01$ mm).

3.4 Photographic Results

Records of impacts were recorded on photographic plates. Each photograph has the nominal impact time in μs written below. The identification was as follows:

Group	Sheet	V_i (m/s)	D_i (mm)	Surface Condition	Image Magnification	View
1	10	25	3	Dry	0.7	Front
	8	25	3	Dry	1.0	Side
2	12	40	3	Dry	0.7	Front
	9	40	3	Dry	1.0	Side
	5	25	5	Wetted	0.6	Front
3	1	25	5	Wetted	0.5	Side
	2	25	5	Wetted	1.2	Side
	3	25	5	Wetted	1.2	Side
4	13	40	3	Wetted	0.6	Front

Unfortunately, the ability to obtain a significant amount of quantitative data from the plates is very limited by the small ejecta diameters. In Figure 11 and 12 are shown typical photographic sequences of the data which is obtained. From the side view photographs, it is easy to estimate that the initial ejecta velocity is of the order of 60 m/s and is at a small angle to the target surface (remember the target is moving at 25 m/s to the right here). There is little hope of estimating droplet size and ejected mass however. Even less information is available from the typical end view sequences shown in Figure 12. Here the non-ejected mass is clearly shown on the center of the target, but again, no quantitative information is easily obtained from this sequence. The photographs do, however, show that

- ejecta droplets have initial velocities which are several times the impact velocity
- splash angles are shallow
- the fact that individual droplets cannot be seen in the photographs indicate that they are on the order of microns or smaller

Negatively, since the data is more *qualitative* than quantitative, the effect of viscosity and surface tension cannot be determined from this experiment or is it likely from similar test programs.

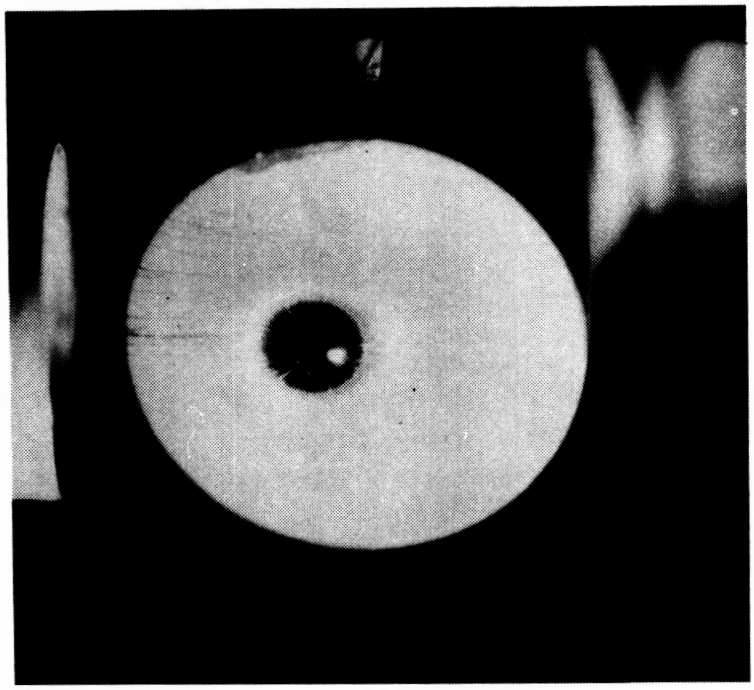

t = 80 μs

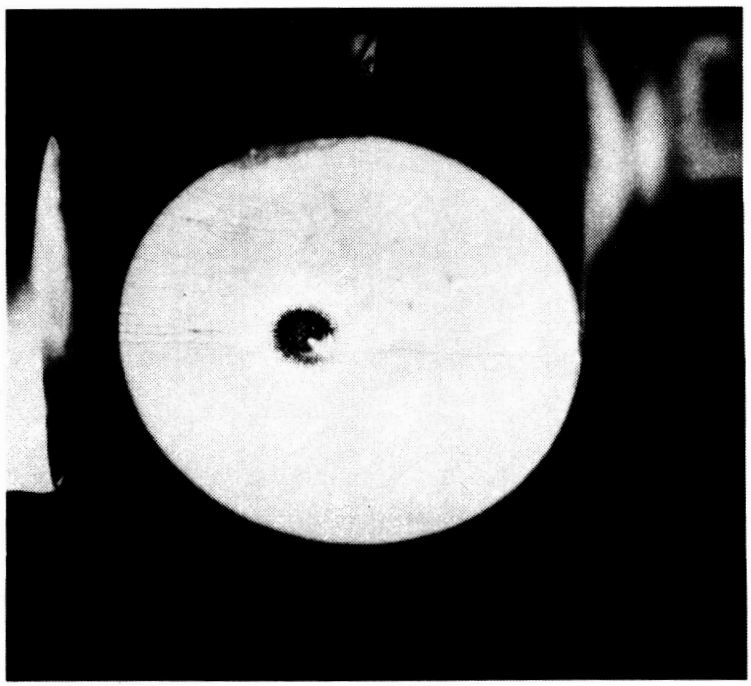

t = 160 μs

Figure 11. Typical time sequenced photographs of normal droplet impact (front view).

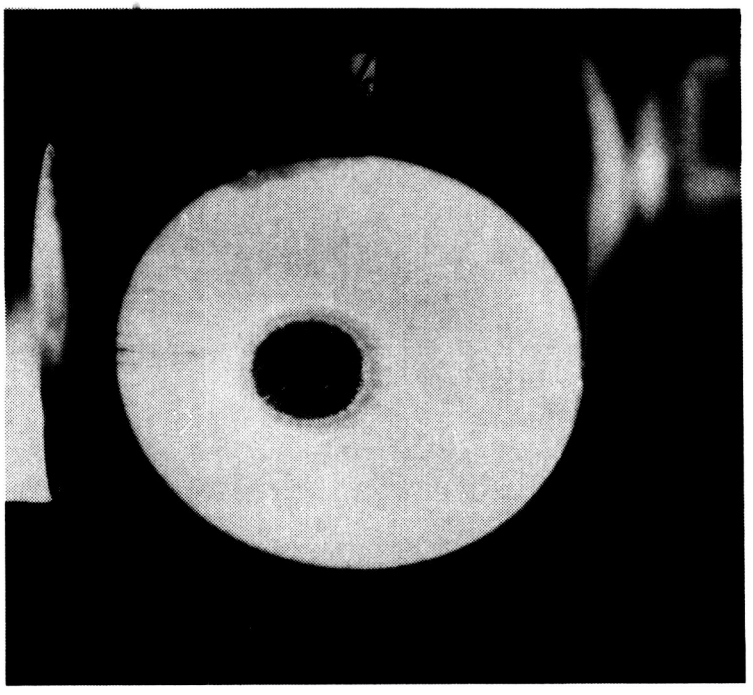

t = 240 μs

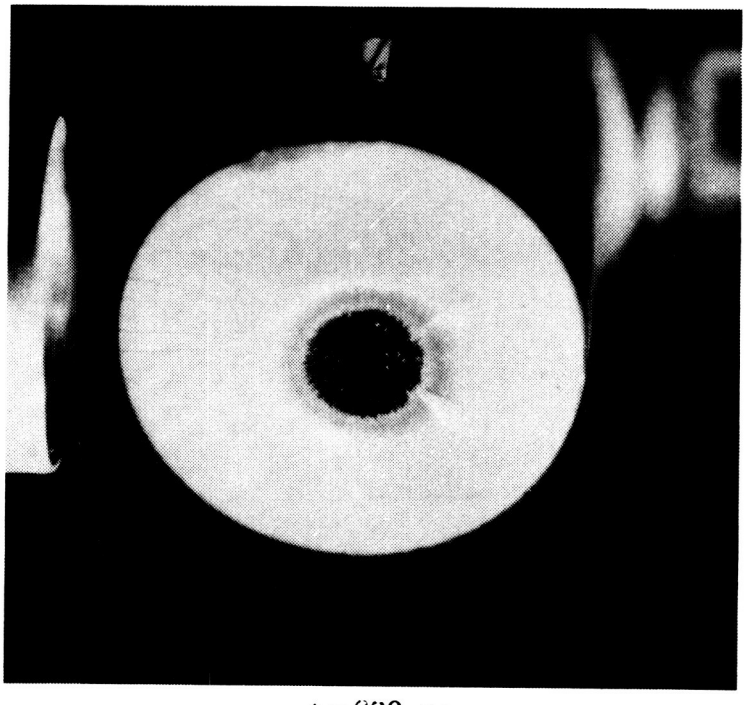

t = 320 μs

Figure 11 (Cont'd). Typical time sequenced photographs of normal droplet impact (front view).

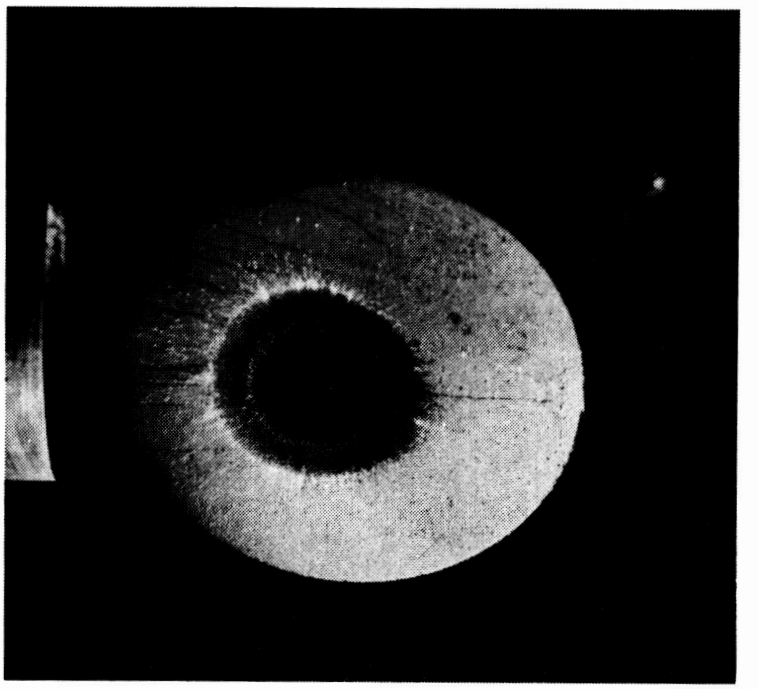

t = 560 μs

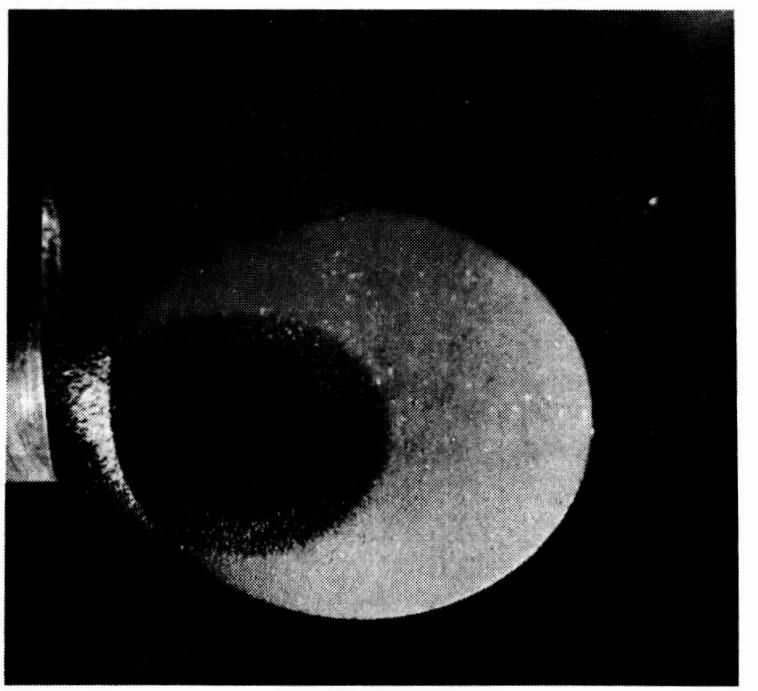

t = 960 μs

Figure 11 (Cont'd). Typical time sequenced photographs of normal droplet impact (front view).

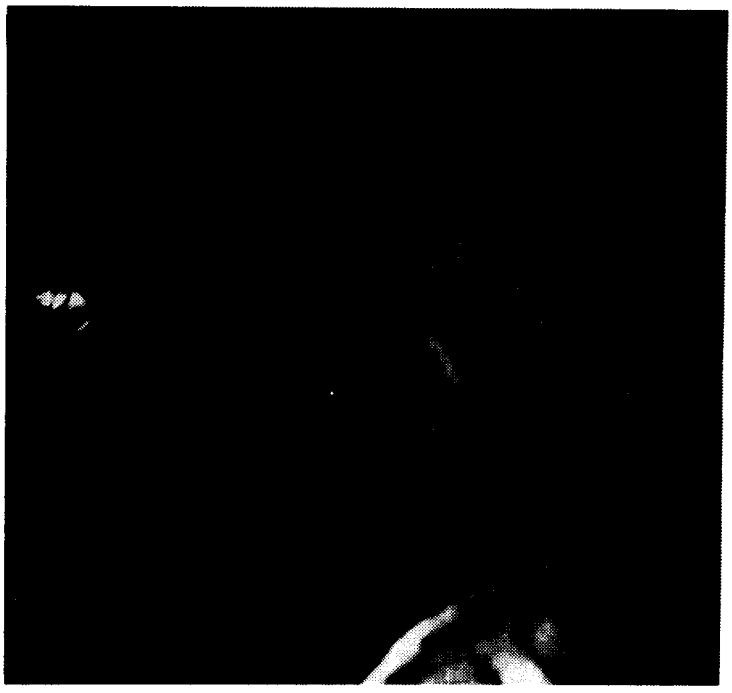

t = 80 μs

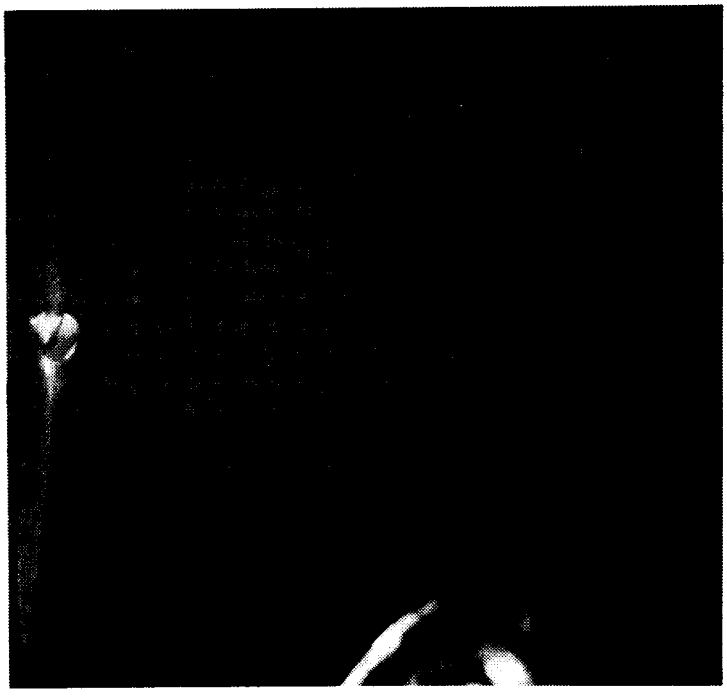

t = 160 μs

Figure 12. Typical time sequenced photographs of normal droplet impact (side view).

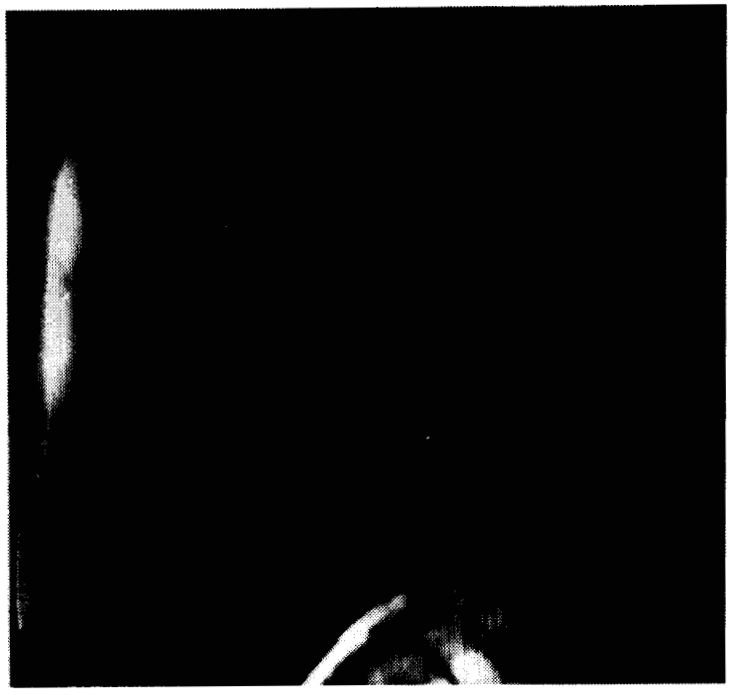

t = 240 μs

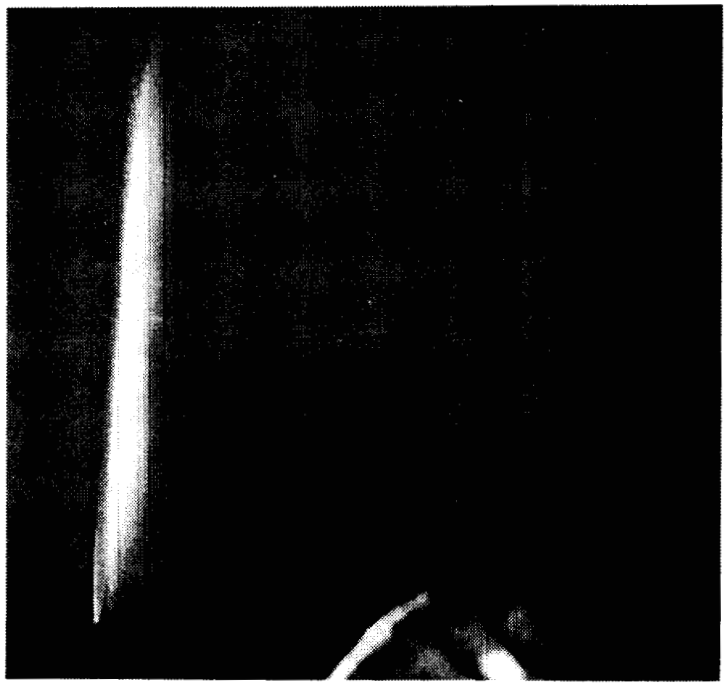

t = 400 μs

Figure 12 (Cont'd). Typical time sequenced photographs of normal droplet impact (side view).

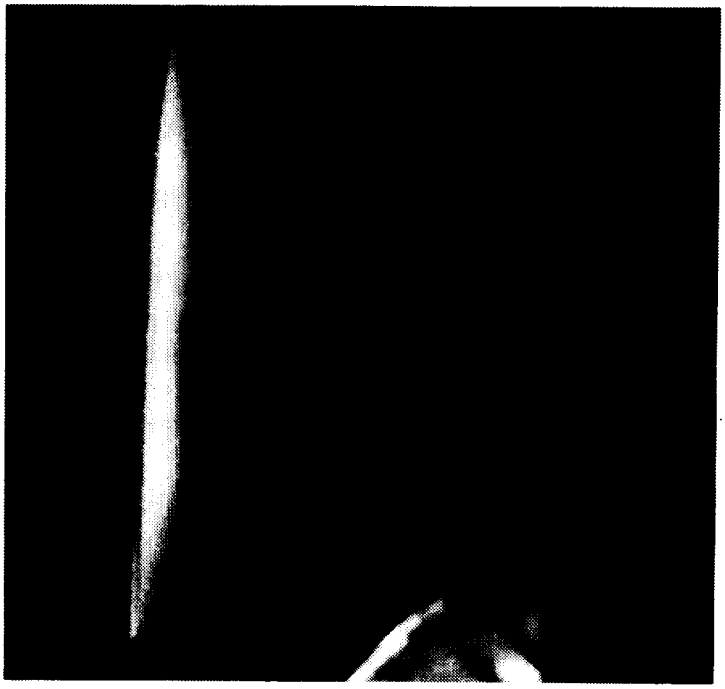

t = 480 μs

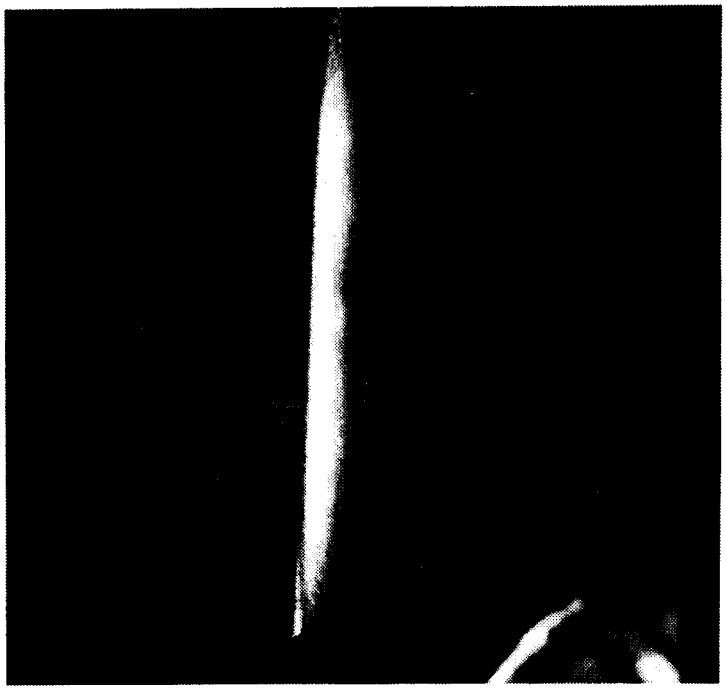

t = 560 μs

Figure 12 (Cont'd). Typical time sequenced photographs of normal droplet impact (side view).

4. CONCLUSIONS

Combined experimental data and analysis suggest that the normal or near normal impact of rain droplets result in an ejecta cloud which is directed along the impacting surface. This cloud is made up of micron-size droplets which represent less than 30% of the impacting mass. The ejecta droplet velocities are initially several times the incoming droplet velocity, but the ejecta are rapidly decelerated by aerodynamic drag forces. The liquid which does not splash back will form an irregular film on the surface of the airfoil complicating the aerodynamic analysis of the airfoil. It is not likely that future research towards modeling droplet impact and splashback will result in the ability to predict airfoil performance degradation from first principles using existing state-of-the-art methods. Complex viscous and surface tension phenomenon at the airfoil surface between the airfoil ejecta and liquid surface film justify fullscale tests to obtain performance degradation data.

5. REFERENCES

1. Bilanin, A. J.: "Proposed Modifications to Ice Accretion/Icing Scaling Theory," AIAA 88-0203, AIAA 26th Aerospace Sciences Meeting, Reno, Nevada, January 1988.

2. Donaldson, C. duP. and Sullivan, R.D.: "An Invariant Second-Order Closure Model of the Compressible Turbulent Boundary Layer on a Flat Plate", Aeronautical Research Associates of Princeton Report No. 178 (NASA CR-128172), June 1972.

3. Lewellen, W.S., Teske, M. E. and Donaldson, C. duP.: "Turbulence Model of Diurnal Variations in the Planetary Boundary Layer", Proceedings of the 1974 Heat Transfer and Fluid Mechanics Institute, Stanford University Press, 1974.

4. Feo, A.: "Single Waterdrop Collision Experiments," Instituto Nacional De Tecnica Aeroespacial Nota Technica No. 221/510/85.009, Madrid Spain, April 1985.

5. Donaldson, C. duP. and Sullivan, R. D.: "The Effect of Heavy Rain on an Airfoil at High Lift," Aeronautical Research Associates of Princeton, Titan Systems Inc. Report No. 597 (NASA CR-178248), 1987.

6. Christie, J. R. I.: " Investigation of the Interaction between Heavy Rainfall and the Boundary Layer: Effects on Aircraft Performance," Princeton University, Department of Mechanical and Aerospace Engineering, Final Report, January 1987.

7. Feo, A. and Gonzalez, P.: "An Experimental Set-Up To Photograhically Record the Impact of Falling Drops on the Leading Edge of an Airfoil Attached to a Rotating Arm," Continuum Dynamics, Inc. Technical Note No. 86-09, October 1986.

8. Feo, A. and Rogles, F.: "Single Drop Perpendicular Impact Experiments," Instituto Nacional De Tecnica Aeroespacial and Continuum Dynamics, Inc. Technical Note 87-04, August 1987.

Appendix A and Appendix B

The following appendices contain subsidiary analyses which were undertaken with support from contract NAS1-18302.

Appendix A

TIME NEEDED

TO WET A FLAT PLATE

IN RAIN

1. INTRODUCTION

An estimate has been made for the length of time required by rain, of a specified liquid water content and incidence angle, falling in a uniform freestream of a known velocity to form a fully developed water film upon a flat plate of a given length.

Calculations were performed for a smooth water film for freestream velocities of 170 and 120 knots (horizontal). The 170 knot calculations cover rain incidence angles, β , of 6°, 12° and 18° and rainfall rates of 50.8 , 254, 762 and 1270 mm/hr. The 120 knot calculations cover the same range of rainfall rates and assume a rain which falls at the same vertical velocity as in the $\beta = 6°$ case of the 170 knot computations.

Additionally, computations were repeated in the 120 knot case for a rough water film.

2. GOVERNING EQUATIONS

The time-dependent governing equations for a water film evolving on a stationary horizontal flat plate which is exposed to rain of a known liquid water content and vertical velocity, falling in a horizontal uniform freestream of a given velocity, can be derived using a control volume consideration similar to that employed in Ref. 1. Neglecting surface tension effects, and applying mass conservation and the streamwise momentum equation for the control volume, the nondimensionalized governing equations can be shown to be as follows:

$$\frac{\partial \delta}{\partial t} = - \frac{\partial}{\partial x} \left(\frac{\delta U}{2}\right) + W_L \sin\beta \qquad (1)$$

$$\frac{\partial}{\partial t} \left(\frac{\delta U}{2}\right) = - \frac{\partial}{\partial x} \left(\frac{\delta U^2}{3}\right) + W_L \sin\beta \cos\beta + \left[\tau(\delta) - \tau(0)\right] \qquad (2)$$

where
- x = distance along the plate
- t = time
- δ = water film thickness
- U = velocity at air/water interface
- W_L = liquid water content (nondimensionalized by density of water)
- β = rain impact angle, between rain trajectory and plate
- $\tau(0)$ = U/δ shear stress at plate surface
- $\tau(\delta)$ = shear stress at air/water interface

The nondimensionalization is performed by using the vertical velocity, density and kinematic viscosity of the rain.

For the smooth film calculations, the shear stress acting on the surface of the film is taken to be that exerted on a smooth flat plate by a turbulent boundary layer (Ref. 2), that is,

$$\tau(\delta) = 0.037\ \rho_a U_a^2 \left[\frac{\nu_a}{U_a(x + x_o)}\right]^{1/5} \qquad (3)$$

where ρ_a , ν_a , U_a are the freestream density, kinematic viscosity and velocity (taken to be horizontal), respectively. The nondimensional length x_o , is evaluated by setting $\tau(\delta) = \tau(0)$ at $x = 0$ and $t = 0$.

Calculations for the case when the film surface is rough employs the shear stress of a turbulent boundary layer on a rough plate (Ref. 2), given by

$$\tau(\delta) = \frac{1}{2}\ \rho_a U_a^2 \left[2.87 + 1.58 \log\left(\frac{x + x_o}{k_s}\right)\right]^{-2.5} \qquad (4)$$

where the roughness height, k_s , is taken to be the water film thickness at the midpoint of the plate computed previously for a smooth film.

3. NUMERICAL METHOD

The governing equations are descretized employing the following explicit scheme which utilizes upwind finite differencing.

$$\delta_i^{n+1} = \delta_i^n - \frac{1}{2}\frac{\Delta t}{\Delta x}\left[(\delta U)_i^n - (\delta U)_{i-1}^n\right] + \Delta t W_L \sin\beta \qquad (5)$$

$$(\delta U)_i^{n+1} = (\delta U)_i^n - \frac{2}{3}\frac{\Delta t}{\Delta x}\left[(\delta U^2)_i^n - (\delta U^2)_{i-1}^n\right] + 2\Delta t\left[\tau^n(\delta) - \tau^n(0)\right]$$
$$+ 2\Delta t W_L \sin\beta \cos\beta \qquad (6)$$

where subscript i denotes evaluation at the i^{th} grid point, superscript n denotes evaluation at the n^{th} time step, Δt is the time step size and Δx is the grid size.

The computation begins with the values of δ and U set suitably small. These values of δ and U are held fixed at the first upstream grid point at $i = 1$ during the time march. The values of δ and δU at all other grid points are calculated at the next time step. The time march terminates when both the relative changes in δ and U, averaged over all grid points and normalized to one characteristic time, are sufficiently small. For the purpose of determining when a steady state solution has been attained in the computations, the characteristic time is taken to be the time taken by the freestream to traverse the plate.

The evolution of the film thickness with time is plotted and the time needed for the film to attain 90% of its final asymptotic thickness is determined. This time will be referred to as the "wetting time" from here on.

4. VERIFICATION OF COMPUTER CODE

Accuracy of the computer code and the underlying numerical method was verified by computing the problem with zero shear stresses. It was shown that the computed and analytical steady state results agree to four significant figures.

5. RESULTS

The wetting time is displayed on Figure 1 for different rainfall rates and rain incidence angles, for a freestream velocity of 87.48 m/s (170 knots). It can be seen that the wetting time decreases approximately hyperbolically with rainfall rate. It also decreases as the rain incidence angle increases.

The wetting time variation with rainfall rate for a slower freestream velocity of 61.73 m/s (120 knots) is displayed in Figure 2. The vertical rain velocity in this case is taken to be identical to that of the case of $\beta = 6^0$ in the 170 knot freestream calculations. Comparison between these two cases for corresponding rainfall rates confirms that in a slower freestream the final film thickness is thicker and the wetting time is longer.

Also exhibited in Figure 2, are the results computed for conditions identical to the above except that the water film is taken to be rough in the sense defined in Section 2. The computed results show that a roughened water film spreads faster and thinner than a smooth film.

The approximation of the shear stress on the film surface by that of the turbulent flat plate boundary layer assumes a no-slip condition at the air/water interface. This approximation can be expected to deteriorate in accuracy as the water film surface velocity increases, as for the case of high rainfall rate and high rain incidence angle. However, even for the 170 knot case, with $\beta = 18°$ and rainfall rate $r = 254$ mm/hr , the highest computed film surface velocity is only about 7% of the freestream, making the no-slip condition a satisfactory engineering approximation for many cases of interest. The highest computed film surface velocity encountered in the present study is about 27% of the freestream, for $\beta = 18°$ and $r = 1270$ mm/hr , for which case the no-slip condition is admittedly crude.

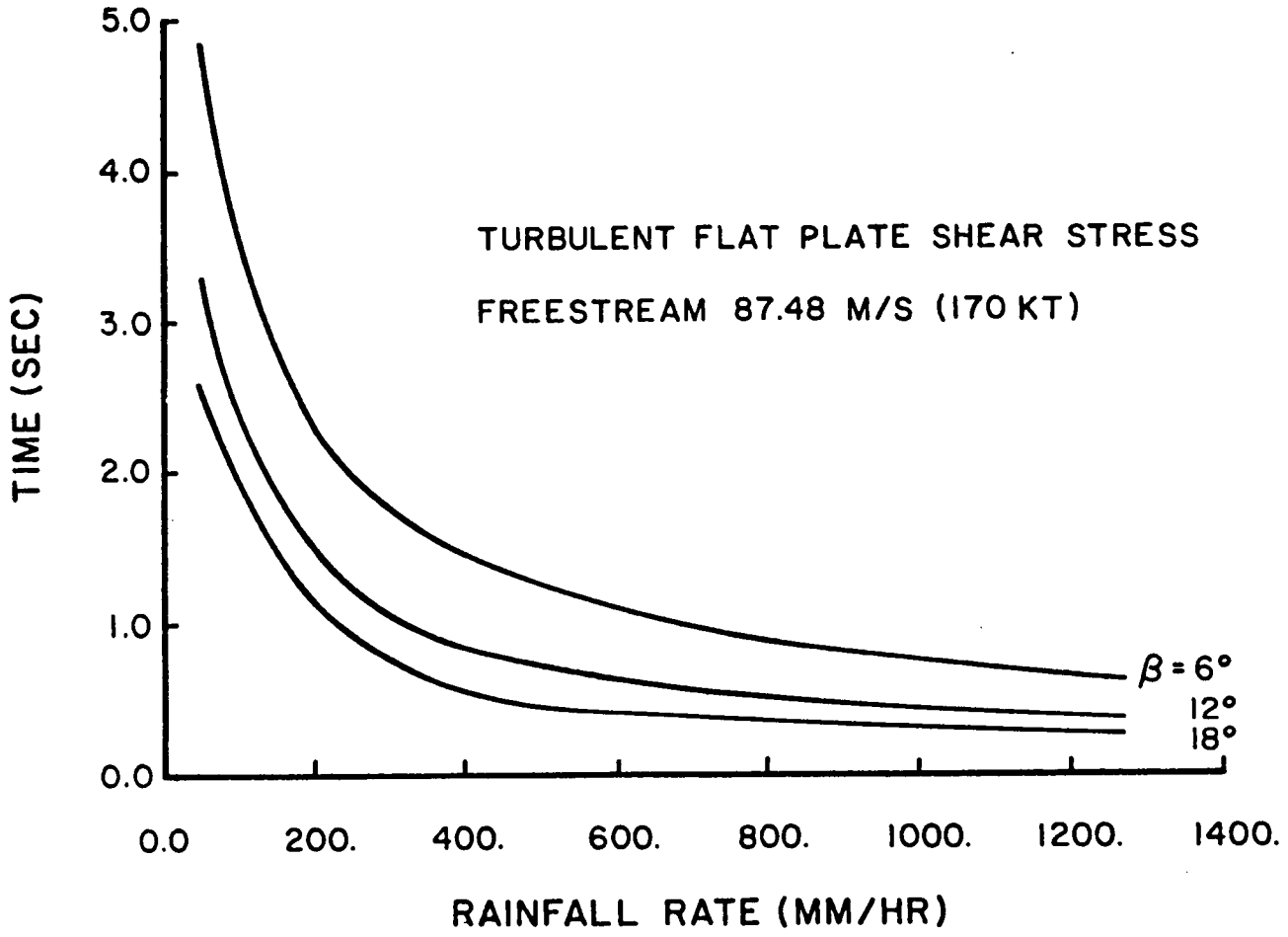

Figure 1. Time to attain 90% of final water film thickness.

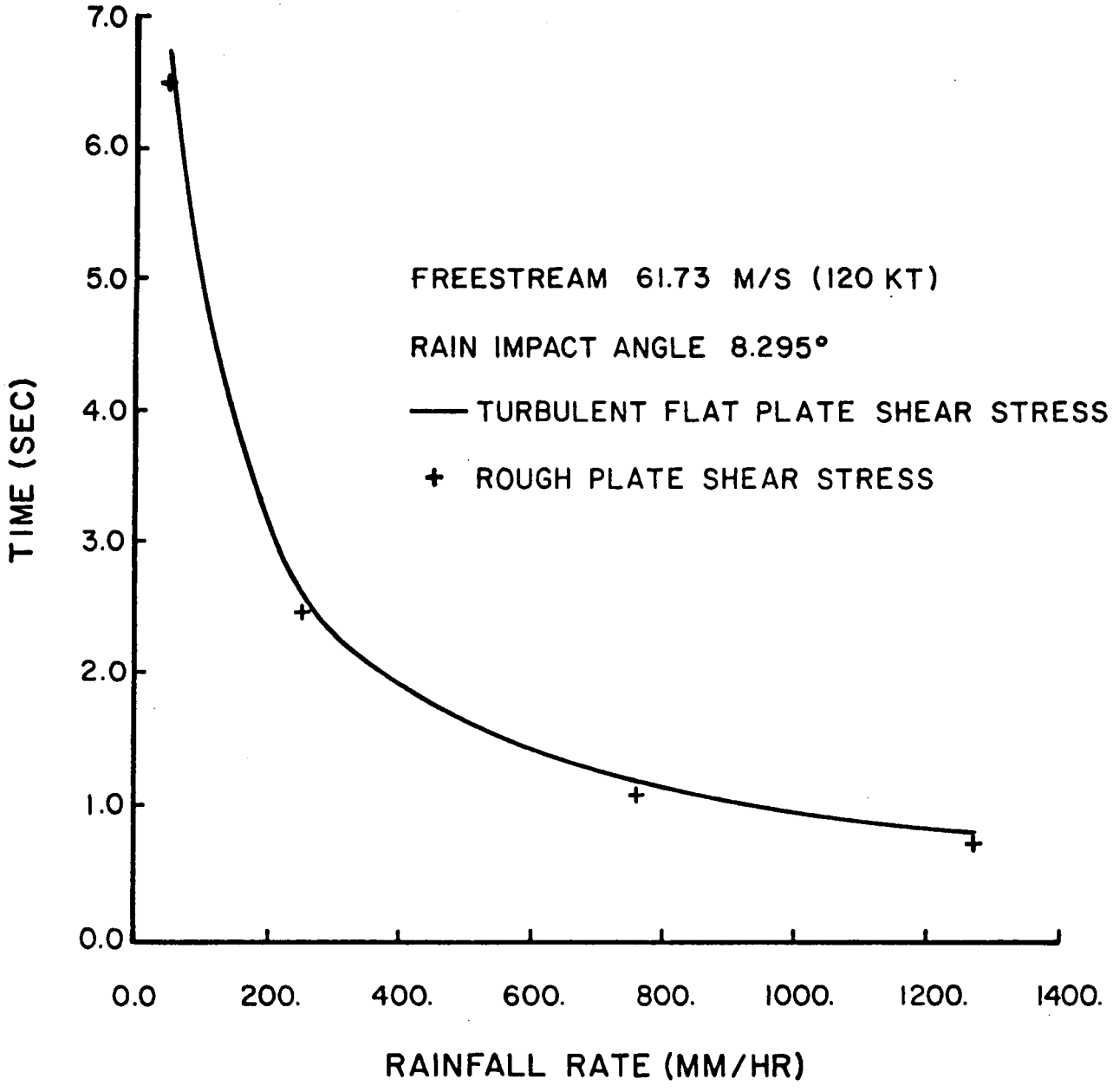

Figure 2. Time to attain 90% of final water film thickness.

6. CONCLUSIONS

The time needed to develop 90% of the final thickness of the water film on a horizontal flat plate, exposed to rain falling with a vertical velocity of 9 m/s in a 120 knot wind, decreases approximately hyperbolically with a rise in rainfall rate, from a value of 6.7 sec at $r = 51.8$ mm/hr to 0.77 sec at $r = 1270$ mm/hr . The corresponding wetting times in a 170 knot wind are 4.9 and 0.62 seconds, respectively.

7. REFERENCES

1. Bilanin, A.J.: "Scaling Laws for Testing of High Lift Airfoils Under Heavy Rainfall," AIAA Paper No. 85-0257 presented at the 23rd Aerospace Sciences Meeting, Reno, Nevada, January 1985.

2. Schlichting, H.: Boundary-Layer Theory, Seventh Edition, McGraw-Hill Book Company, 1979.

NASA
National Aeronautics and Space Administration

Report Documentation Page

1. Report No.	2. Government Accession No.	3. Recipient's Catalog No.
NASA CR-181842		

4. Title and Subtitle

Feasibility of Predicting Performance Degradation of Airfoils in Heavy Rain

5. Report Date

June 1989

6. Performing Organization Code

7. Author(s)

A. J. Bilanin, T. R. Quackenbush, and A. Feo

8. Performing Organization Report No.

C.D.I. Report No. 89-04

10. Work Unit No.

505-68-01

9. Performing Organization Name and Address

Continuum Dynamics, Inc.
P. O. Box 3073
Princeton, New Jersey 08540

11. Contract or Grant No.

NAS1-18302

13. Type of Report and Period Covered

Contractor Report

12. Sponsoring Agency Name and Address

National Aeronautics & Space Administration
Langley Research Center
Hampton, VA 23665-5225

14. Sponsoring Agency Code

15. Supplementary Notes

Langley Research Center - R. Earl Dunham
Final Report Technical Advisor

16. Abstract

The following report documents the effort undertaken by Continuum Dynamics, Inc. on behalf of NASA Langley in support of the heavy rain aerodynamic performance penalty program. This effort supported the design of a fullscale test program as well as examined the feasibility of estimating the degradation of performance of airfoils from first principles. The analytic efforts were supplemented by a droplet splashback test program in an attempt to observe the physics of impact and generation of ejecta. These tests demonstrated that the interaction of rain with an airfoil is a highly complex phenomenon and this interaction is not likely to be analyzed analytically with existing tools.

17. Key Words (Suggested by Author(s))	18. Distribution Statement
Heavy Rain, Splashback, Thin Film Layer Droplet Impact	Unclassified - Unlimited Subject Category 02

19. Security Classif. (of this report)	20. Security Classif. (of this page)	21. No. of pages	22. Price
Unclassified	Unclassified	56	A04